Original article

NRJ

The Neuroradiology Journal
2017, Vol. 30(6) 535–545

DOI: 10.1177/1971400917739273
journals.sagepub.com/home/neu

SAGE

Longitudinal evaluation of resting-state connectivity, white matter integrity and cortical thickness in stable HIV infection: Preliminary results

Diogo G Corrêa[1,2], Nicolle Zimmermann[1,3], Nina Ventura[2,4], Gustavo Tukamoto[2], Thomas Doring[2], Sarah CB Leite[1], Rochele P Fonseca[1,3], Paulo RV Bahia[1], Fernanda CR Lopes[2,4] and Emerson L Gasparetto[1,2]

Abstract

Purpose: The objectives of this study were to determine if HIV-infected patients treated with highly active antiretroviral therapy (HAART), without dementia, suffer from longitudinal gray matter (GM) volume loss, changes in white matter (WM) integrity and deterioration in functional connectivity at rest, in an average interval of 30 months.

Methods: Clinically stable HIV-positive patients (on HAART, CD4 + T lymphocyte > 200 cells/μl, and viral loads <50 copies/μl) were recruited. None of them had HIV-associated dementia. Each patient underwent two scans, performed in a 1.5-T magnetic resonance imaging (MRI) scanner. FreeSurfer was used to perform cortical volumetric reconstruction and segmentation of GM structures. WM integrity was assessed using tract-based spatial statistics to post-process diffusion tensor imaging data, and FMRIB's Software Library tools were used to post-process resting-state functional magnetic resonance imaging (RS-fMRI).

Results: There were no significant differences in cortical thickness, deep GM volumes, or diffusivity parameters between the scans at the two time points. Five resting-state networks were identified in our patients. In the second MRI, HIV-positive patients presented increased areas of functional connectivity in visual pathways, frontoparietal and cerebellar networks, compared with the first MRI (considering $p < 0.05$).

Conclusions: RS-fMRI revealed potentially compensatory longitudinal alterations in the brains of HIV-positive patients, attempting to compensate for brain damage related to the infection.

Keywords

HIV, cortical thickness, diffusion tensor imaging, resting-state functional imaging, longitudinal follow-up

Introduction

The pandemic of human immunodeficiency virus (HIV) infection is entering its fourth decade, with an estimated 35.3 million people living with HIV around the world.[1] Although there is still no definitive cure or efficacy-confirmed vaccine, HIV-infection can be treated effectively with highly active antiretroviral therapy (HAART). Owing to HAART's effectiveness, HIV-infected patients are living longer. However, even with HAART, the life expectancy of HIV-infected patients is shorter than noninfected controls.[2]

Cognitive dysfunction in HIV-positive patients may reflect irreversible brain damage.[3] Among people currently living with a long-term HIV-treatment regimen, manifestation of HIV-associated neurocognitive disorders (HAND) is typically subtler than in the pre-HAART era, though still of serious morbidity concern.[3] In the majority of cases, HAND are characterized by asymptomatic neurocognitive impairment,

[1]Department of Radiology, Hospital Universitário Clementino Fraga Filho, Federal University of Rio de Janeiro, Brazil
[2]Clínica de Diagnóstico por Imagem (CDPI), Brazil
[3]Department of Psychology, Pontifical Catholic University of Rio Grande do Sul, Brazil
[4]Department of Radiology, Hospital Universitário Antônio Pedro, Federal Fluminense University, Brazil

Corresponding author:
Diogo Goulart Corrêa, Hospital Universitário Clementino Fraga Filho, Rua Rodolpho Paulo Rocco 255, Cidade Universitária, Ilha do Fundão, Rio de Janeiro, RJ, 21941913, Brazil.
Email: diogogoulartcorrea@yahoo.com.br

which can emerge even in patients with an undetectable viral load.[4]

Diffusion tensor imaging (DTI) measures the directional nature of water diffusion through cellular structures, such as myelin and white matter (WM) tracts, which can differ between normal and pathological tissue.[5] Many researchers have found decreased fractional anisotropy (FA) and increased mean diffusivity (MD) and radial diffusivity (RD) in WM regions of HIV-infected patients.[6–8] Significant differences in basal ganglia volume and cortical thickness have been observed between HIV-positive patients and controls.[9–11] However, the large overlap of values between patients and controls prevents the definitive use of these techniques in clinical practice.[6,7]

Resting-state functional magnetic resonance imaging (RS-fMRI) measures spontaneous low-frequency fluctuations in blood oxygen level-dependent (BOLD) signals at rest, enabling investigation of the brain's functional architecture.[12,13] In general, previous studies have found reduced connectivity in some neural networks, such as the default mode, salience, executive, and lateral occipital networks,[14–16] in HIV-infected patients, considering patients with detectable viral loads[14–16] and patients without HAART.[15,16]

Because advanced MRI techniques can detect early differences between HIV-positive and control groups, they may reveal signs of premature deterioration over the course of a longitudinal follow-up study. Such findings could stimulate changes in antiretroviral therapy plans and the introduction of cognitive therapy, with the aim of reducing morbidity.

The objectives of this study were to determine if HIV-positive patients on HAART, without dementia, suffer from longitudinal gray matter (GM) volume loss, changes in WM integrity and deterioration in functional connectivity at rest, during an average interval of 30 months.

Materials and methods

Participants

The institutional review board approved this study and all participants signed an informed consent. Between September 2009 and September 2015, 12 patients with HIV infection, confirmed by enzyme-linked immunosorbent assay and Western blot, were selected from the University Hospital database. On the week of the first MRI, all patients were on stable HAART and had viral load <50 copies/μl and CD4 + T lymphocyte >200 cells/μl. Exclusion criteria included declared illicit drug use within the past year, neurological disorders such as current or past central nervous system infection, MRI contra-indications, and clinically significant abnormal brain magnetic resonance imaging (MRI) findings in conventional sequences, as determined by a neuroradiologist (15 years' experience).

The cohort included 10 men and two women (mean age 52.8 years, range 44–59 years) with an average of 9.6 years of education (range, 5–20 years). They had an average illness duration of 15.6 years (range, 5–24 years), undetectable plasma viral loads and an average CD4 + T lymphocyte count of 723.6 cells/μl (range, 406–1164 cells/μl). All 12 patients received HAART throughout our study (Table 1); among them, six patients were rated as 0.0 on the Memorial Sloan Kettering (MSK) ratio, three had a MSK rating of 0.5, three had a MSK rating of 1.0, and none had a MSK rating ≥ 2.0.[17]

A battery of neuropsychological tests, in accordance with the recommendations of Antinori et al.,[17] was used to characterize the cognitive profiles of the participants on the day of their first MRI examinations. A neuropsychologist with eight years' experience administered the tests (N.Z.). The battery consisted of standard tests that were adapted and interpreted according to normative demographic data from a Brazilian population (Table 2). Six of the 12 patients did not have HAND, four had HIV-associated asymptomatic neurocognitive impairment, two had HIV-associated mild neurocognitive disorder, and none had HIV-associated dementia. Specifically, deficits were observed in memory ($n = 4$), executive function ($n = 4$), processing speed ($n = 3$), and motor and sensory-perceptual skills ($n = 1$). None of our patients exhibited deficits in the domains of verbal language or attention/working memory.

The participants underwent two MRI examinations with an average interval of 30.4 months (range, 12–49 months; median, 28.14 months). At the time of the second MRI, all patients were on the same antiretroviral regimen, and maintained CD4 + T lymphocyte counts >200 cells/μl (average of 721.83 cells/μl, ranging from 520 to 1125 cells/μl) and undetectable plasma viral loads and consistent MSK ratings.

MRI acquisition

MRI was performed with a 1.5-T scanner (Avanto, Siemens, Erlangen, Germany) using an eight-channel phased-array head coil. The MRI protocol included: axial fluid-attenuation inversion recovery (repetition time (TR) = 9000 ms; echo time (TE) = 83 ms; field of view (FOV) = 230 mm; matrix = 244 × 256; section thickness = 4.5 mm with a 10% gap; flip angle = 180 degrees; inversion time = 2500 ms); sagittal T1-three-dimensional (3D) magnetization-prepared rapid gradient echo (MPRAGE) weighted-image (TR = 2730 ms; TE = 3.26 ms; inversion time = 1000 ms; FOV = 256 mm; matrix = 192 × 256; section thickness = 1.3 mm, flip angle = 7 degrees; voxel size = 1.3 × 1.0 × 1.3 mm). Axial diffusion tensor single-shot echo-planar imaging was acquired using bipolar diffusion gradients applied along 30 noncollinear directions (b0 = 0 and b1 = 900 s/mm^2) (TR = 10100 ms; TE = 94 ms; FOV = 256 mm; matrix = 122 × 120; 65 slices with 2.1 mm thickness and no gap). A 6-minute RS-fMRI

Table 1. Antiretroviral schemes used by the participants and the central nervous system (CNS)-penetration effectiveness score

Antiretroviral therapy	Number of patients using the scheme	CNS penetration-effectiveness score
Zidovudine + lamivudine + efavirenz	3	9
Zidovudine + lamivudine + atazanavir/ritonavir	3	8
Zidovudine + lamivudine + tenofovir + efavirenz	1	10
Zidovudine + lamivudine + fosamprenavir/ritonavir	1	9
Zidovudine + lamivudine + tenofovir + lopinavir/ritonavir	1	10
Tenofovir + lamivudine + efavirenz	1	6
Zidovudine + tenofovir + darunavir/ritonavir	1	8
Lamivudine + tenofovir + fosamprenavir/ritonavir	1	6

Table 2. Cognitive domains examined, tests used and the considered variables in each test.

Cognitive domains	Neuropsychological tests	Variables
Attention/working memory	Bells Cancellation test	Omissions (time 1)
	Hayling test and Trail Making test	Errors (part A)
	Wechsler Adult Intelligence Scale – III	Digits forward and backward and letter-number sequencing tasks
Memory (learning, recall)	Rey auditory verbal learning test	Mean of A1 and B1 trials; mean of A7, B1 and A5 trial
Sensory-perceptual and motor skills domains	Brazilian Brief Neuropsychological assessment battery (NEUPSILIN)	Constructive praxis task
Processing speed	Bells cancellation test	Omission (time 1)
	Hayling test and Trail Making test	Time (part A)
Executive functions	Stroop test	Color-word page; interference score
	Trail Making test	Time (part B); errors (part B); Time B-Time A; Time B/Time A
	Hayling test	Errors part B; Time B-Time A
Verbal language	Montreal Communication Evaluation Battery	Semantic and phonemic verbal fluency tasks.

was acquired with a T2*-weighted echo-planar imaging sequence, sensitive to the BOLD contrast (TR = 3290 ms; TE = 30 ms; flip angle = 85 degrees, matrix = 72 × 72; FOV = 100 mm; 124 images with 3-mm thickness and 30% gap; one average). Participants were instructed to remain awake, keep their eyes closed, and think of nothing in particular while MRI was being performed. Their heads were stabilized with tape across the forehead and padding around the sides. All MRI images were reviewed by an experienced neuroradiologist with 15 years' experience (E.L.G) and were of good quality for post-processing.

Cortical thickness, volumetric measures and statistical analysis

Cortical reconstruction and volumetric segmentation was performed using FreeSurfer software (version 5.3.0; http://surfer.nmr.mgh.harvard.edu) with sagittal T1-3D MPRAGE-weighted images. Technical details of these procedures have been described previously.[18,19] Briefly, the processing included removal of non-brain tissue by way of a hybrid watershed/surface deformation procedure, followed by segmentation of subcortical WM and deep GM structures. Motion correction, automated Talairach transformation, normalization of intensity, tessellation of GM/WM boundaries, and automated topology correction were then performed. Finally, GM/WM and GM/cerebrospinal fluid (CSF) borders were placed at the location where the greatest shift in intensity defines these transitions. The pial surface was generated by expanding the WM surface, so that it followed the GM-CSF intensity gradient closely, without crossing the WM surface boundary. If the surface appeared to deviate from the GM/CSF boundary, manual editing was performed.

Cortical thickness maps were developed for each participant at each time point. Cortical thickness was adjusted for age and gender. All the cortical regions were considered, as shown in Figure 1. Corrections for multiple comparisons were performed by query design estimate contrast, using Monte-Carlo simulation, available in FreeSurfer, and mean cortical

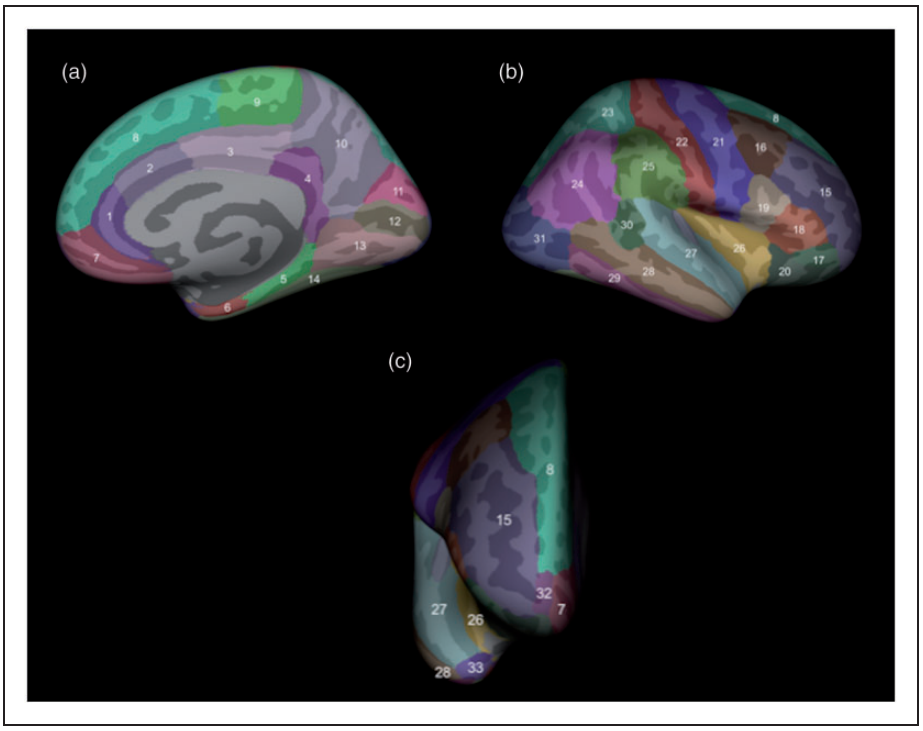

Figure 1. Assessment of cortical thickness in brain areas, as shown in this three-dimensional rendering from medial (a), lateral (b) and frontal (c) views. The cortical structures assessed, delineated by FreeSurfer, were the rostral (1) and caudal (2) anterior cingulate gyrus, posterior cingulate gyrus (3), isthmus of the cingulate gyrus (4), parahippocampal gyrus (5), entorhinal cortex (6), medial orbitofrontal cortex (7), superior frontal gyrus (8), paracentral lobule (9), precuneus (10), cuneus (11), pericalcarine cortex (12), lingual gyrus (13), fusiform gyrus (14), rostral (15) and caudal (16) middle frontal gyrus, pars orbitalis (17), pars triangularis (18) and pars opercularis (19) of the inferior frontal gyrus, lateral orbitofrontal cortex (20), precentral gyrus (21), postcentral gyrus (22), superior (23) and inferior (24) parietal cortex, supramarginal gyrus (25), insular cortex (26), superior temporal gyrus (27), middle temporal gyrus (28), inferior temporal gyrus (29), banks of the superior temporal sulcus (30), lateral occipital cortex (31), frontal pole (32) and temporal pole (33).

thickness was compared between the first and second MRIs (considering $p < 0.05$).

Using the same technique, the volumes of the following structures were measured automatically: thalamus, caudate, putamen, globus pallidum, accumbens, hippocampus, and amygdala. These volumes were corrected for head size by dividing each value by the cranial volume and multiplying the result by 100. Normality of deep GM volume distributions was tested with the Kolmogorov-Smirnov test. All the regions considered had a normal distribution of their volumes. Differences in deep GM volumes were tested with paired sample *t*-test (significance at $p < 0.05$). We also measured the correlation between the time interval between the MRIs and the volume of the deep GM structures.

Post-processing of WM integrity evaluation and statistical analysis

For voxelwise diffusion modeling, diffusion data were analyzed using FMRIB's Diffusion Toolbox within FSL 5.0 (http://www.fmrib.ox.ac.uk/fsl).[20] After performing eddy current correction and brain extraction, FA images for all participants were created by fitting a tensor model onto the raw diffusion data. Voxelwise statistical analysis of the FA data was carried out using tract-based spatial statistics (TBSS),[21] part of the FSL program. Briefly, FA data for all individuals were aligned in a common space using the nonlinear registration tool FNIRT, which uses a b-spline representation of the registration warp field. Next, the mean FA image was created and thinned to create a mean FA skeleton, which represents the centers of all tracts common to the group. Aligned FA data for each individual were then projected onto this skeleton, and the resulting data were fed into voxelwise cross-subject statistics for all voxels with FA $\geq$0.30 to exclude peripheral tracts with significant inter-subject variability and/or partial GM volume effects. By applying the original nonlinear registration of each participant's FA to a standard space, the RD, MD and axial diffusivity (AD) were also projected onto the mean FA skeleton.

To perform the longitudinal statistical analysis, the differences between the diffusion data of the first MRI and the corresponding second MRI acquisition of each participant were manually computed. The resultant difference values were fed into one-sample paired *t*-tests, with permutation-based inference (5000 permutations), corrected for multiple comparisons (controlling the family-wise error) with threshold-free cluster enhancement and significance level of $p < 0.05$. The results were overlaid on the mean FA skeleton to identify possible altered areas in the main tracts, based on the Johns Hopkins University WM tractography atlas and the

International Consortium for Brain Mapping DTI-81 WM labels atlas, both available within FSL.

Post-processing of RS-fMRI and statistical analysis

RS-fMRI data were post-processed with FMRIB's Software Library tools (http://www.fmrib.ox.ac.uk/fsl), using a methodology previously described.[22] The images were motion-corrected and non-brain tissue was removed. In addition, the images were spatially smoothed and temporally filtered. After this preprocessing, functional scans were aligned to a T1 3D MPRAGE-weighted image and then to the Montreal Neurological Institute (MNI)-152 standard space by way of nonlinear registration. The aligned data were temporally concatenated across participants to create a single four-dimensional dataset, which was decomposed using independent component analysis (ICA) to identify large-scale functional connectivity patterns.[23] Next, between-subjects' analysis was carried out with a "dual-regression" approach that allows for voxelwise comparisons. The functional networks were selected by visual inspection and comparison to earlier studies.[12,13] Voxelwise group differences were detected with a general linear model and nonparametric permutation testing (5000 permutations). Multiple comparisons were controlled for in the resultant spatial maps (significance at $p < 0.05$) with threshold-free cluster enhancement.

Cortical and subcortical areas were identified based on the Harvard-Oxford Cortical Structural Atlas and Harvard-Oxford Subcortical Structural Atlas (both in FSL).

Results

Cortical thickness and deep GM structures volume

No significant differences in cortical thickness were observed between the first and second MRI scans in the HIV-positive patients group.

There were also no significant differences in mean deep GM structures volumes between the first and second MRIs (Table 3).

There was no significant correlation between time and volumes of deep GM structures (Table 3).

WM integrity

There were no significant differences in mean FA, RD, MD or AD values of WM tracts between the first and second MRIs in HIV-positive patients.

Functional connectivity at rest

Thirty-five components were computed in the entire participant group by ICA. Five of these components coincided with resting-state networks described in previous studies (visual network, with areas of dorsal attention; frontoparietal network; executive network; default mode network; cerebellar, with areas of thalamic network).

Table 3. Comparative analysis of mean volumes of the deep GM structures, corrected by the skull volume, between the first and second MRIs and correlation coefficient between time and deep GM volume. There were no statistically significant differences in the volume of deep GM structures considered, nor a correlation between the time interval and volume of the anatomical structures considered.

Anatomical structures		First MRI (standard deviation)	Second MRI (standard deviation)	*p* value of the comparative analysis between the first and second MRIs[a]	Pearson correlation coefficient between time and volume[b] (*p* value)
Thalamus	Left	0.4433 (0.0518)	0.4342 (0.0483)	0.0819	0.3694 (0.2372)
	Right	0.4314 (0.0467)	0.4234 (0.0502)	0.1139	0.3305 (0.2939)
Caudate	Left	0.2065 (0.0230)	0.2055 (0.0225)	0.5831	−0.2426 (0.4474)
	Right	0.2234 (0.0254)	0.2243 (0.0185)	0.7537	−0.0933 (0.7730)
Putamen	Left	0.3622 (0.0517)	0.3524 (0.0485)	0.0825	0.4738 (0.1197)
	Right	0.3520 (0.0448)	0.3458 (0.0442)	0.0563	0.3855 (0.2158)
Globus pallidum	Left	0.1045 (0.0136)	0.0986 (0.0109)	0.0738	0.3768 (0.2272)
	Right	0.0995 (0.0132)	0.0952 (0.0078)	0.1217	0.5655 (0.0553)
Accumbens	Left	0.0395 (0.0087)	0.0416 (0.0090)	0.2067	0.5267 (0.0784)
	Right	0.0376 (0.0075)	0.0374 (0.0096)	0.9295	0.3417 (0.2769)
Hippocampus	Left	0.2421 (0.0359)	0.2483 (0.0355)	0.2528	0.3367 (0.2845)
	Right	0.2457 (0.0333)	0.2496 (0.0355)	0.3154	0.1890 (0.5561)
Amygdala	Left	0.0929 (0.0148)	0.0967 (0.0124)	0.2967	−0.0091 (0.9776)
	Right	0.1027 (0.0150)	0.1066 (0.0139)	0.2144	0.2269 (0.4780)

Statistical tests used: [a]Student's *t*-test for paired samples; [b]Pearson correlation test.
GM: gray matter; MRI: magnetic resonance imaging.

There were no significant differences in the executive network and in the default mode network, between the two MRI time points.

There were cortical areas in the visual network that exhibited greater mean connectivity at the second MRI, compared to the first. Specifically, the difference involved voxels in the bilateral posterior cingulate gyrus, bilateral pericalcarine cortex, bilateral precuneus, bilateral lingual gyrus, bilateral occipital pole, bilateral cuneus, left parietal cortex, left postcentral gyrus, left supramarginal gyrus, and right hippocampus (Figure 2).

In the frontoparietal network, increased mean connectivity values in the second MRI were observed in few voxels, compared to the first MRI, including some in the left precentral gyrus, left superior parietal cortex, left lateral occipital cortex, right precuneus, right parietal cortex, and right lateral occipital cortex (Figure 3).

The second MRI presented areas with increased mean connectivity, compared to the first MRI, in the cerebellar network, including voxels throughout the vermis and within the cerebellar hemispheres (Figure 4).

None of the resting-state networks identified presented areas of decreased connectivity in the second MRI, compared to the first MRI.

Discussion

In this longitudinal study, we used voxel-based techniques to assess cortical thickness and deep GM volumes, DTI to assess WM integrity, and RS-fMRI to assess functional connectivity in HIV-positive patients without dementia, who were on stable HAART, with CD4 + T lymphocyte counts > 200 cells/μl and undetectable plasma viral loads. No longitudinal differences in cortical thickness, deep GM structures volumes, or WM diffusivity parameters were observed. However, from the first to the second MRI scan, performed at an average interval of 30.4 months, we found areas of increased mean connectivity values, at rest, in the visual, frontoparietal, and cerebellar networks. To the best of our knowledge, this is the first study to evaluate cortical thickness, deep GM volumes, DTI parameters and RS-fMRI, longitudinally, in the same HIV-infected patients.

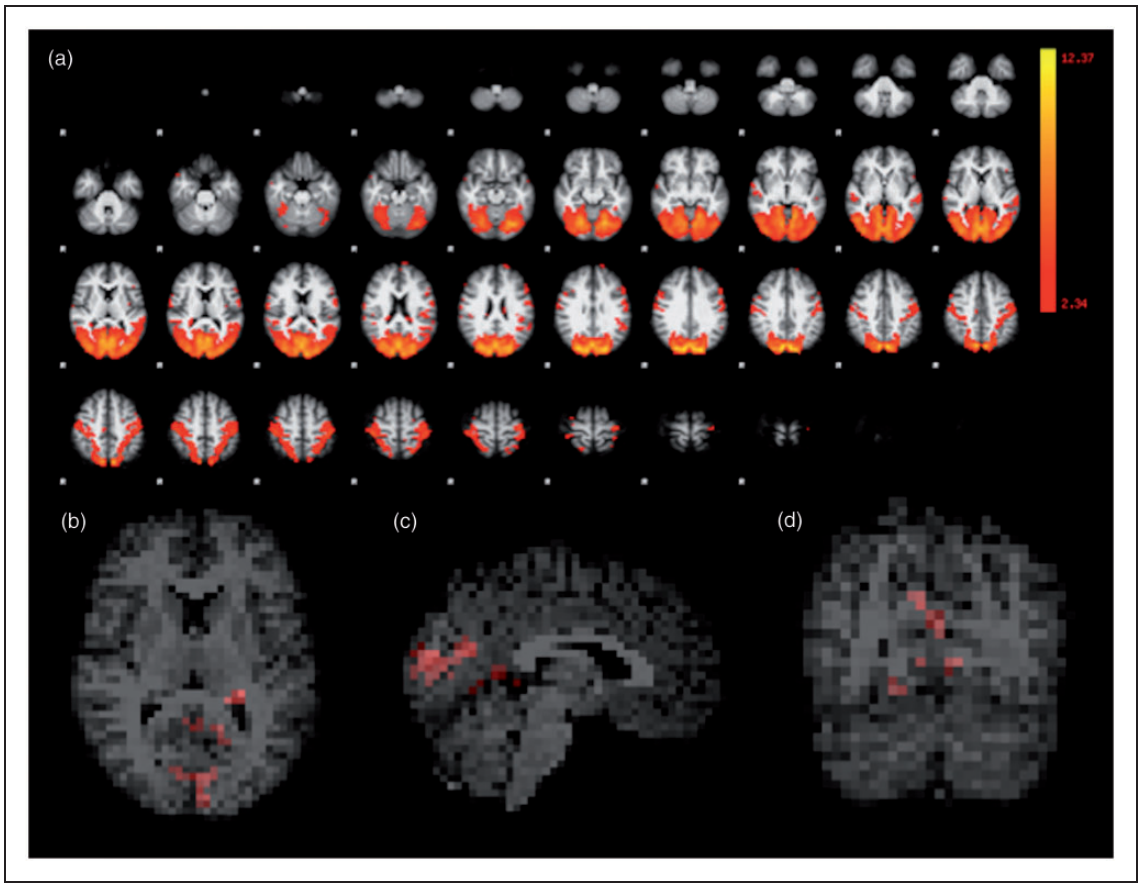

Figure 2. Visual network, with areas of dorsal attention, functional representation. All first and second MRI scans were considered in the ICA (a). Corrected RS-fMRI maps in the axial (b), sagittal (c), and coronal (d) planes, comparing the second vs. the first MRI of the HIV-positive participants. Red voxels in (b), (c) and (d) represent areas with increased mean connectivity at the second MRI vs. the first, encompassing much of the occipital lobes, in this network. MRI: magnetic resonance imaging; ICA: independent component analysis; RS-fMRI: resting-state functional magnetic resonance imaging; HIV: human immunodeficiency virus.

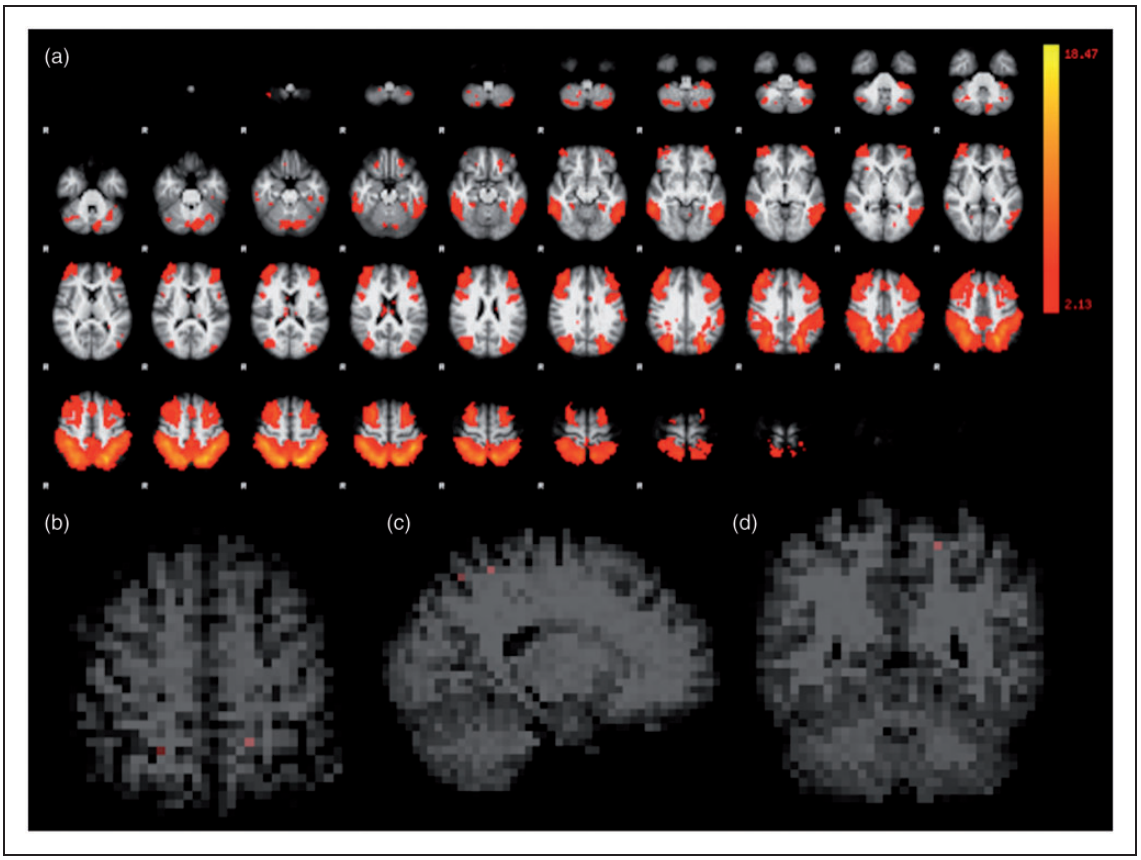

Figure 3. Frontoparietal network functional representation. All first and second MRI scans were considered in the ICA (a). Corrected RS-fMRI maps in the axial (b), sagittal (c), and coronal (d) planes comparing the second vs. the first MRI of the HIV-positive participants. Red voxels in (b), (c) and (d) represent few areas with increased mean connectivity at the second MRI, in this network. MRI: magnetic resonance imaging; ICA: independent component analysis; RS-fMRI: resting-state functional magnetic resonance imaging; HIV: human immunodeficiency virus.

Despite having normal visual acuity, HIV-infected patients, with or without neurological symptoms, may have dysfunction of the optic nerves/retrochiasmal visual pathways, due to direct effects of the virus or in combination with other cofactors.[24] The frontoparietal network includes the lateral prefrontal cortex and the inferior parietal lobule, which are activated during tasks requiring cognitive control or executive function.[25] In the post-HAART era, executive dysfunctions are detected in approximately half of HIV-infected individuals with neurocognitive impairment, which emerge early and tend to worsen with disease progression.[26] Classically considered to be a motor coordination center, the cerebellum is increasingly being recognized for its involvement in cognitive processing.[27] Previous studies have reported associations between HIV infection and cerebellar neuronal death.[28] The present findings of increased connectivity in visual, frontoparietal, and cerebellar networks over time are consistent with these previous studies. We hypothesize that the increased connectivity observed may be related to neural compensation for brain damage.

Aging-exacerbated volume reduction of various brain areas in HIV-infected patients has been reported, including the superior temporal, inferior frontal, medial temporal, and cingulate cortices,[29] as well as reductions of medial and superior frontal gyri,[30] caudate nucleus,[31,32] amygdala and corpus callosum.[31] Aging-related changes in the 3D morphometry of bilateral accumbens, amygdala, caudate and thalamus, as well as right pallidum and right putamen, have also been reported in HIV-positive patients.[33] Pfefferbaum et al.,[34] in a longitudinal study, found that HIV-positive patients presented with a greater decrease in insula and hippocampus volume and a greater increase in lateral ventricles volume, compared to controls. Additionally, these authors also found HIV infection and age-related acceleration in the decrease of frontal, sensorimotor and temporoparietal cortices and in the thalamus volumes.[34] Decreased FA in the posterior limbs of the internal capsules, cerebral peduncles, and anterior corona radiata of HIV-positive patients has been related to aging.[35] Other authors found a significant increase in mean MD in the genu of the corpus callosum after one year.[36] However, the samples in these previous studies were heterogeneous in terms of treatment, viral load, and CD4 + T lymphocyte level.[32–36] In the present study, HIV-positive patients did not show longitudinal changes in cortical thickness, deep GM volumes and diffusivity parameters. Similarly, two

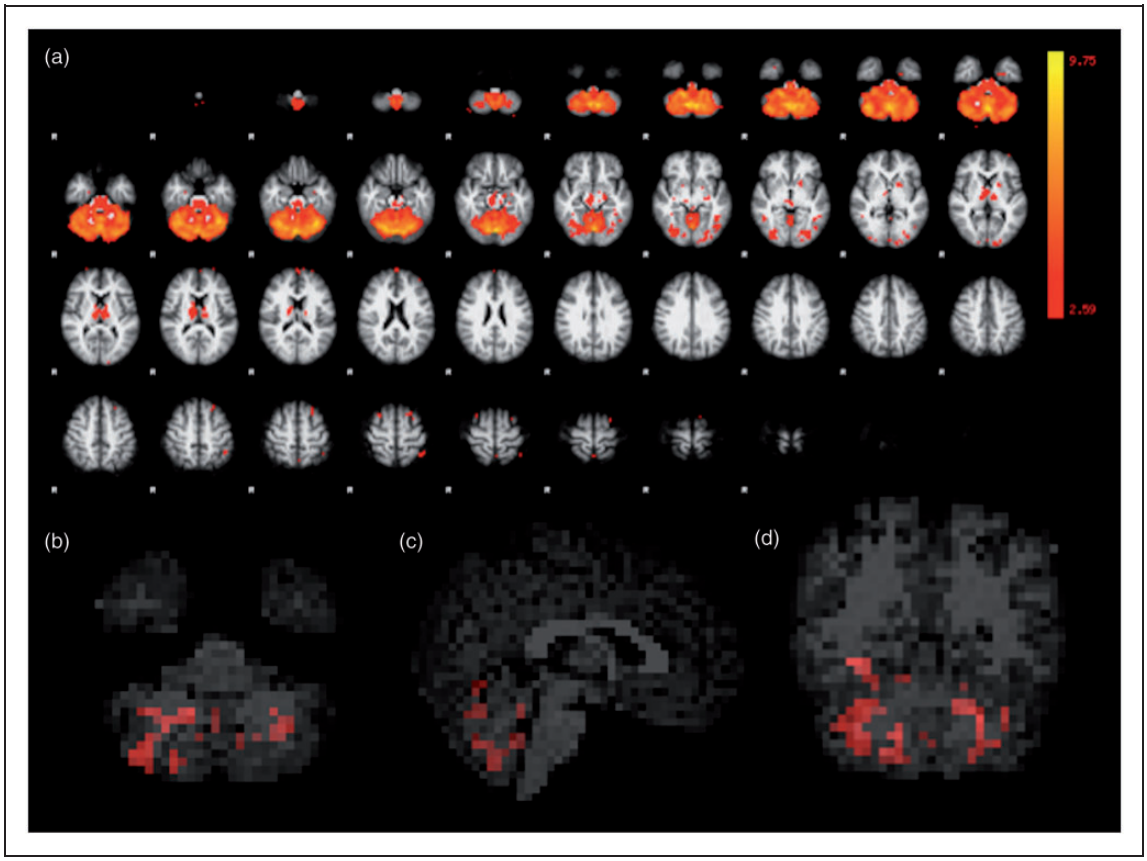

Figure 4. Functional representation of cerebellar, with areas of thalamic, network. All first and second MRI scans were considered in the ICA (a). Corrected RS-fMRI maps in the axial (b), sagittal (c), and coronal (d) planes, comparing the second vs. the first MRI of the HIV-positive participants. Red voxels in (b), (c) and (d) represent areas with increased mean connectivity at the second MRI, encompassing the cerebellar vermis and hemispheres, in this network. MRI: magnetic resonance imaging; ICA: independent component analysis; RS-fMRI: resting-state functional magnetic resonance imaging; HIV: human immunodeficiency virus.

previous studies did not find longitudinal changes in these parameters, in HIV-positive patients on a stable HAART regimen with undetectable viral loads and CD4 + T lymphocyte > 200 cells/μl.[31,37] Therefore, we hypothesize that the stable treatment and good clinical parameters of our patients may have reduced the sensitivity of cortical thickness and subcortical GM volume measurement, as well as DTI parameters, to detect brain deterioration of the participants. Also, our study has a relatively short duration of follow-up, since the mean interval between the MRIs was 30 months and other authors conducted a longer follow-up.[34]

Previous cross-sectional studies assessing RS-fMRI in HIV-positive patients have found decreased connectivity within the default mode, control, and salience networks[16] and between the striatum and the default mode and ventral attention networks.[15] Decreased bilateral connectivity between the precuneus and prefrontal cortex has been reported in HIV patients with HAND compared with those without HAND. Decreased bilateral connectivity between the precuneus and the cerebellum, frontal lobes and temporal lobes was also found in HIV-positive patients without HAND compared to HIV-negative controls.[38] Additionally, HIV-infected patients over 60 years old with detectable plasma HIV-RNA levels were found to have decreased connectivity within the salience network compared to that in HIV-infected individuals in whom HIV-RNA was not detectable.[14] Furthermore, reduced connectivity in the left inferior parietal cortex within the lateral occipital cortex network has been reported to correlate with visual-motor coordination task performance, indicating changes in resting-state functional connectivity of visual pathways.[39] Conversely, higher connectivity has been observed between the striatum and the default mode network and ventral attention network in HIV patients using HAART, compared with the connectivity observed in those not using HAART.[15] Unlike these previous cross-sectional studies, in the current study, we evaluated longitudinal changes, comparing the same patients at two time points (mean interval, 30.4 months). Notwithstanding, the aforementioned previous studies also found changes in the connectivity of visual,[39] cerebellar,[38] and frontoparietal,[14,16] areas, since the salience network has patterns of intrinsic cortical and subcortical connectivity from the lateral frontoparietal central executive network,[40] suggesting that HIV-positive patients are prone to develop lesions in these areas.

Thomas et al.[16] observed no interactions between HIV status and aging in RS-fMRI connectivity. However, in that study, not all patients were on treatment or had an undetectable viral load. Conversely, Chang et al.[41] found increased activation in the left posterior attention network in older, cognitively normal HIV-positive patients during the performance of low attentional-load tasks, and further found increased activation in the left posterior and anterior attention network during the performance of higher attentional-load tasks. Ernst et al.[42] used fMRI, during a set of visual attention tasks, to assess brain activation longitudinally in neurocognitively normal HIV-infected patients over a one-year period. The participants showed no longitudinal change in task performance, but they showed significant connectivity increases in prefrontal and posterior parietal cortices during the performance of more difficult tasks in the second MRI, relative to the levels seen one year earlier, in the first scan. Although the current study evaluates RS-fMRI and these previous studies evaluated connectivity during visual attention tasks, our results show some similarities, since they found increased longitudinal connectivity in certain brain areas in patients with stable HIV infection. These results support the hypothesis that increases in brain connectivity in RS-fMRI may occur in an attempt to maintain brain function, despite ongoing injury, even in well-managed HIV-positive patients.

The mechanisms responsible for the increased longitudinal connectivity in the HIV-positive patients are unclear. However, our findings suggest that brain injury continues, despite well-controlled viral load and CD4 + T lymphocyte counts. It may have happened because of continued neuroinflammation, with glial activation, which is present even in patients with well-controlled systemic immune status[43] and/or it may be mediated by ongoing injury to the dopaminergic system, which plays a major role in regulating visual pathways[44] and cognition[45] and has been implicated in HAND.[46] These mechanisms may progressively reduce the efficiency of the neural substrate, necessitating HIV-positive patients to compensate by increasing brain activation.[42] Another hypothesis for our results could be the treatment effect, since previous studies suggest an increase in brain activation of HIV-positive patients using HAART, compared to untreated patients and controls.[15,47,48] In the current study, all participants were under HAART. So, we could not conclude whether the longitudinal differences in brain connectivity were caused by HIV infection itself or by the treatment, or even by a combination of them.

Although our study used a relatively small sample, we assessed patients with specific clinical conditions, all with CD4 + T lymphocyte > 200 cells/μl, undetectable viral loads, without dementia and on stable HAART regimens. Additionally, prior relevant studies using fMRI in HIV infection have reported smaller samples.[49,50] Also, we could not compare subgroups distinguished by neurocognitive impairment severity. Nevertheless, it is noteworthy that patients can fluctuate between non-HAND and asymptomatic neurocognitive impairment. Furthermore, current definitions for HIV-associated asymptomatic neurocognitive impairment and mild neurocognitive disorder might be too inclusive and lead to clinical inflation of impairment data.[51] Although we have not included a control group in our study, it did not influence our results. A potential limitation of the study is the use of anisotropic voxels in 3D-T1 MPRAGE-weighted images, which may limit the measurement of cortical thickness. However, we used the same exam protocol in all MRIs performed, with a great test reliability.[52] Even though there is an age-related decline in GM volume[53] and DTI parameters[54] in healthy individuals, no significant longitudinal differences in these parameters are expected in supposedly healthy individuals in an interval of 30.4 months. Also, a decrease in functional connectivity during healthy aging is expected;[41,55] however, our results showed a longitudinal increase in functional connectivity in some networks. Furthermore, ICA-derived spatial maps of resting state networks, as conducted in this study, do not require a prior hypothesis[13] and are unaffected by respiratory/cardiac fluctuations.[56] Thus, our results are sufficient to demonstrate that HIV-positive patients without dementia develop areas of increased brain connectivity over time, attempting to compensate for brain damage caused by HIV infection itself, rather than aging.

Conclusion

RS-fMRI is useful for detecting longitudinal alterations in the brains of clinically stable HIV-positive patients under treatment, which may reflect compensation for brain damage, caused by the infection, or/and an effect of HAART on the brain. Changes in brain structure, such as cortical thickness and WM tract changes, were not detectable in HIV-positive patients by the presently used methods within the time frame of the current study.

Funding

This research received no specific grant from any funding agency in the public, commercial, or not-for-profit sectors.

Conflict of interest

The authors declared no potential conflicts of interest with respect to the research, authorship, and/or publication of this article.

References

1. Maartens G, Celum C and Lewin SR. HIV infection: Epidemiology, pathogenesis, treatment, and prevention. *Lancet* 2014; 384: 258–271.
2. Deeks SG and Phillips AN. HIV infection, antiretroviral treatment, ageing, and non-AIDS related morbidity. *BMJ* 2009; 338: a3172.

3. Spudich S. HIV and neurocognitive dysfunction. *Curr HIV/AIDS Rep* 2013; 10: 235–243.
4. Simioni S, Cavassini M, Annoni JM, et al. Cognitive dysfunction in HIV patients despite long-standing suppression of viremia. *AIDS* 2010; 24: 1243–1250.
5. Dong Q, Welsh RC, Chenevert TL, et al. Clinical applications of diffusion tensor imaging. *J Magn Reson Imaging* 2004; 19: 6–18.
6. Ragin AB, Storey P, Cohen BA, et al. Whole brain diffusion tensor imaging in HIV-associated cognitive impairment. *AJNR Am J Neuroradiol* 2004; 25: 195–200.
7. Leite SC, Corrêa DG, Doring TM, et al. Diffusion tensor MRI evaluation of the corona radiata, cingulate gyri, and corpus callosum in HIV patients. *J Magn Reson Imaging* 2013; 38: 1488–1493.
8. Corrêa DG, Zimmermann N, Doring TM, et al. Diffusion tensor MR imaging of white matter integrity in HIV-positive patients with planning deficits. *Neuroradiology* 2015; 57: 475–482.
9. Thompson PM, Dutton RA, Hayashi KM, et al. Thinning of the cerebral cortex visualized in HIV/AIDS reflects CD4 + T lymphocyte decline. *Proc Natl Acad Sci U S A* 2005; 102: 15647–15652.
10. Ragin AB, Du H, Ochs R, et al. Structural brain alterations can be detected early in HIV infection. *Neurology* 2012; 79: 2328–2334.
11. Corrêa DG, Zimmermann N, Netto TM, et al. Regional cerebral gray matter volume in HIV-positive patients with executive function deficits. *J Neuroimaging* 2016; 26: 450–457.
12. Lee MH and Smyser CD and Shimony JS. Resting-state fMRI: A review of methods and clinical applications. *AJNR Am J Neuroradiol* 2013; 34: 1866–1872.
13. Smitha KA, Akhil Raja K, Arun KM, et al. Resting state fMRI: A review on methods in resting state connectivity analysis and resting state networks. *Neuroradiol J* 2017; 30: 305–317.
14. Guha A, Wang L, Tanenbaum A, et al. Intrinsic network connectivity abnormalities in HIV-infected individuals over age 60. *J Neurovirol* 2016; 22: 80–87.
15. Ortega M, Brier MR and Ances BM. Effects of HIV and combination antiretroviral therapy on cortico-striatal functional connectivity. *AIDS* 2015; 29: 703–712.
16. Thomas JB, Brier MR, Snyder AZ, et al. Pathways to neurodegeneration: Effects of HIV and aging on resting-state functional connectivity. *Neurology* 2013; 80: 1186–1193.
17. Antinori A, Arendt G, Becker JT, et al. Updated research nosology for HIV-associated neurocognitive disorders. *Neurology* 2007; 69: 1789–1799.
18. Fischl B, Salat DH, Busa E, et al. Whole brain segmentation: Automated labeling of neuroanatomical structures in the human brain. *Neuron* 2002; 33: 341–355.
19. Desikan RS, Ségonne F, Fischl B, et al. An automated labeling system for subdividing the human cerebral cortex on MRI scans into gyral based regions of interest. *Neuroimage* 2006; 31: 968–980.
20. Smith SM, Jenkinson M, Woolrich MW, et al. Advances in functional and structural MR image analysis and implementation as FSL. *Neuroimage* 2004; 23(Suppl 1): S208–S219.
21. Smith SM, Jenkinson M, Johansen-Berg H, et al. Tract-based spatial statistics: Voxelwise analysis of multi-subject diffusion data. *Neuroimage* 2006; 31: 1487–1505.
22. Roosendaal SD, Schoonheim MM, Hulst HE, et al. Resting state networks change in clinically isolated syndrome. *Brain* 2010; 133(Pt 6): 1612–1621.
23. Beckmann CF, DeLuca M, Devlin JT, et al. Investigations into resting-state connectivity using independent component analysis. *Philos Trans R Soc Lond B Biol Sci* 2005; 360: 1001–1013.
24. Mwanza JC, Nyamabo LK, Tylleskär T, et al. Neuro-ophthalmological disorders in HIV infected subjects with neurological manifestations. *Br J Ophthalmol* 2004; 88: 1455–1459.
25. Vincent JL, Kahn I, Snyder AZ, et al. Evidence for a frontoparietal control system revealed by intrinsic functional connectivity. *J Neurophysiol* 2008; 100: 3328–3342.
26. Woods SP, Moore DJ, Weber E, et al. Cognitive neuropsychology of HIV-associated neurocognitive disorders. *Neuropsychol Rev* 2009; 19: 152–168.
27. Stoodley CJ and Schmahmann JD. Evidence for topographic organization in the cerebellum of motor control versus cognitive and affective processing. *Cortex* 2010; 46: 831–844.
28. Kwakwa HA and Ghobrial MW. Primary cerebellar degeneration and HIV. *Arch Intern Med* 2001; 161: 1555–1556.
29. Becker JT, Maruca V, Kingsley LA, et al. Factors affecting brain structure in men with HIV disease in the post-HAART era. *Neuroradiology* 2012; 54: 113–121.
30. Towgood KJ, Pitkanen M, Kulasegaram R, et al. Mapping the brain in younger and older asymptomatic HIV-1 men: Frontal volume changes in the absence of other cortical or diffusion tensor abnormalities. *Cortex* 2012; 48: 230–241.
31. Ances BM, Ortega M, Vaida F, et al. Independent effects of HIV, aging, and HAART on brain volumetric measures. *J Acquir Immune Defic Syndr* 2012; 59: 469–477.
32. Stout JC, Ellis RJ, Jernigan TL, et al. Progressive cerebral volume loss in human immunodeficiency virus infection: A longitudinal volumetric magnetic resonance imaging study. *Arch Neurol* 1998; 55: 161–168.
33. Kuhn T, Schonfeld D, Sayegh P, et al. The effects of HIV and aging on subcortical shape alterations: A 3D morphometric study. *Hum Brain Mapp* 2017; 38: 1025–1037.
34. Pfefferbaum A, Rogosa DA, Rosenbloom MJ, et al. Accelerated aging of selective brain structures in human immunodeficiency virus infection: A controlled, longitudinal magnetic resonance imaging study. *Neurobiol Aging* 2014; 35: 1755–1768.
35. Seider TR, Gongvatana A, Woods AJ, et al. Age exacerbates HIV-associated white matter abnormalities. *J Neurovirol* 2016; 22: 201–212.
36. Chang L, Wong V, Nakama H, et al. Greater than age-related changes in brain diffusion of HIV patients after 1 year. *J Neuroimmune Pharmacol* 2008; 3: 265–274.
37. Corrêa DG, Zimmermann N, Tukamoto G, et al. Longitudinal assessment of subcortical gray matter volume, cortical thickness, and white matter integrity in HIV-positive patients. *J Magn Reson Imaging* 2016; 44: 1262–1269.
38. Ann HW, Jun S, Shin NY, et al. Characteristics of resting-state functional connectivity in HIV-associated neurocognitive disorder. *PLoS One* 2016; 11: e0153493.
39. Wang X, Foryt P, Ochs R, et al. Abnormalities in resting-state functional connectivity in early human immunodeficiency virus infection. *Brain Connect* 2011; 1: 207–217.

40. Seeley WW, Menon V, Schatzberg AF, et al. Dissociable intrinsic connectivity networks for salience processing and executive control. *J Neurosci* 2007; 27: 2349–2356.
41. Chang L, Holt JL, Yakupov R, et al. Lower cognitive reserve in the aging human immunodeficiency virus-infected brain. *Neurobiol Aging* 2013; 34: 1240–1253.
42. Ernst T, Yakupov R, Nakama H, et al. Declined neural efficiency in cognitively stable human immunodeficiency virus patients. *Ann Neurol* 2009; 65: 316–325.
43. Bell JE, Arango JC and Anthony IC. Neurobiology of multiple insults: HIV-1-associated brain disorders in those who use illicit drugs. *J Neuroimmune Pharmacol* 2006; 1: 182–191.
44. Brandies R and Yehuda S. The possible role of retinal dopaminergic system in visual performance. *Neurosci Biobehav Rev* 2008; 32: 611–656.
45. Störmer VS, Passow S, Biesenack J, et al. Dopaminergic and cholinergic modulations of visual-spatial attention and working memory: Insights from molecular genetic research and implications for adult cognitive development. *Dev Psychol* 2012; 48: 875–889.
46. Wang GJ, Chang L, Volkow ND, et al. Decreased brain dopaminergic transporters in HIV-associated dementia patients. *Brain* 2004; 127: 2452–2458.
47. Chang L, Yakupov R, Nakama H, et al. Antiretroviral treatment is associated with increased attentional load-dependent brain activation in HIV patients. *J Neuroimmune Pharmacol* 2008; 3: 95–104.
48. Ances BM, Roc AC, Korczykowski M, et al. Combination antiretroviral therapy modulates the blood oxygen level-dependent amplitude in human immunodeficiency virus-seropositive patients. *J Neurovirol* 2008; 14: 418–424.
49. Ernst T, Chang L, Jovicich J, et al. Abnormal brain activation on functional MRI in cognitively asymptomatic HIV patients. *Neurology* 2002; 59: 1343–1349.
50. Melrose RJ, Tinaz S, Castelo JM, et al. Compromised fronto-striatal functioning in HIV: An fMRI investigation of semantic event sequencing. *Behav Brain Res* 2008; 188: 337–347.
51. Clifford DB and Ances BM. HIV-associated neurocognitive disorder. *Lancet Infect Dis* 2013; 13: 976–986.
52. Wonderlick JS, Ziegler DA, Hosseini-Varnamkhasti P, et al. Reliability of MRI-derived cortical and subcortical morphometric measures: Effects of pulse sequence, voxel geometry, and parallel imaging. *Neuroimage* 2009; 44: 1324–1333.
53. Inano S, Takao H, Hayashi N, et al. Effects of age and gender on neuroanatomical volumes. *J Magn Reson Imaging* 2013; 37: 1072–1076.
54. Madden DJ, Spaniol J, Costello MC, et al. Cerebral white matter integrity mediates adult age differences in cognitive performance. *J Cogn Neurosci* 2009; 21: 289–302.
55. Damoiseaux JS, Beckmann CF, Arigita EJ, et al. Reduced resting-state brain activity in the "default network" in normal aging. *Cereb Cortex* 2008; 18: 1856–1864.
56. Beckmann CF, DeLuca M, Devlin JT, et al. Investigations into resting-state connectivity using independent component analysis. *Philos Trans R Soc Lond B Biol Sci* 2005; 360: 1001–1013.